

PAPER • OPEN ACCESS

Entropy production along nonequilibrium quantum jump trajectories

To cite this article: Jordan M Horowitz and Juan M R Parrondo 2013 *New J. Phys.* **15** 085028

View the [article online](#) for updates and enhancements.

You may also like

- [Super-additivity in communication of classical information through quantum channels from a quantum parameter estimation perspective](#)
Jan Czajkowski, Marcin Jarzyna and Rafa Demkowicz-Dobrzanski
- [Phenomenology of buoyancy-driven turbulence: recent results](#)
Mahendra K Verma, Abhishek Kumar and Amrishi Pandey
- [HEATING OF THE SOLAR CHROMOSPHERE AND CORONA BY ALFVÉN WAVE TURBULENCE](#)
A. A. van Ballegoijen, M. Asgari-Targhi, S. R. Cranmer et al.

Entropy production along nonequilibrium quantum jump trajectories

Jordan M Horowitz^{1,3} and Juan M R Parrondo²

¹ Department of Physics, University of Massachusetts at Boston, Boston, MA 02125, USA

² Departamento de Física Atómica, Molecular y Nuclear and GISC, Universidad Complutense de Madrid, E-28040 Madrid, Spain
E-mail: jordan.horowitz@umb.edu

New Journal of Physics **15** (2013) 085028 (23pp)

Received 23 May 2013

Published 27 August 2013

Online at <http://www.njp.org/>

doi:10.1088/1367-2630/15/8/085028

Abstract. For classical nonequilibrium systems, the separation of the total entropy production into the adiabatic and nonadiabatic contributions is useful for understanding irreversibility in nonequilibrium thermodynamics. In this paper, we formulate quantum analogues for driven open quantum systems describable by quantum jump trajectories by applying a quantum stochastic thermodynamics. Our main conclusions are based on a quantum formulation of the local detailed balance condition.

³ Author to whom any correspondence should be addressed.



Content from this work may be used under the terms of the [Creative Commons Attribution 3.0 licence](https://creativecommons.org/licenses/by/3.0/). Any further distribution of this work must maintain attribution to the author(s) and the title of the work, journal citation and DOI.

Contents

1. Introduction	2
2. Setup	4
2.1. Repeated interaction framework	4
2.2. Quantum thermodynamic process	4
3. Total entropy production with repeated interactions	6
4. Entropy production for quantum jump trajectories	7
4.1. Effective dynamics and the stochastic master equation	8
4.2. Local detailed balance	9
4.3. Total entropy production	10
5. Nonadiabatic and adiabatic entropy productions	11
5.1. Dual process	12
5.2. Nonadiabatic and adiabatic entropy productions	13
6. Illustrations	13
6.1. Coherent thermal reservoir	14
6.2. Driven harmonic oscillator	16
7. Conclusion	17
Acknowledgments	19
Appendix A. Effective dynamics for short interactions	19
Appendix B. Operators for dual quantum Markov processes	21
References	22

1. Introduction

Entropy production has been customarily split into two pieces, a part due to the system ΔS and a contribution from the environment ΔS_{env} : $\Delta S_{\text{tot}} = \Delta S + \Delta S_{\text{env}}$ [1]. However, the development and subsequent analysis of the fluctuation theorems testify to the value of a distinct decomposition into adiabatic ΔS_a and nonadiabatic ΔS_{na} contributions [2–5]:

$$\Delta S_{\text{tot}} = \Delta S_a + \Delta S_{\text{na}}. \quad (1)$$

The nomenclature emphasizes that for an adiabatic (slow) process—during which the system remains in its instantaneous stationary state— $\Delta S_{\text{na}} = 0$, and all of the entropy production is due to the adiabatic component, $\Delta S_{\text{tot}} = \Delta S_a$. Far from being a simple recasting, this decomposition provides a refined understanding of irreversibility in nonequilibrium processes [6]. Both ΔS_a and ΔS_{na} are individually always positive (on average), unlike ΔS and ΔS_{env} . Equation (1) is particularly useful when applied to stationary states that support dissipative currents. In this case, ΔS_a quantifies the entropy production needed to maintain these currents. Whereas, for transitions between stationary states, ΔS_{na} is a measure of irreversibility that remains finite in the limit of slow switching; ΔS_{tot} and ΔS_a are essentially useless, as they diverge due to the continuous dissipation present in nonequilibrium stationary states.

Remarkably, each of these entropy productions satisfies a detailed fluctuation theorem on the level of individual, fluctuating, microscopic trajectories. Namely, the change in trajectory-dependent total entropy ΔS_{tot} , nonadiabatic entropy ΔS_{na} and adiabatic entropy ΔS_a , can be

deduced by comparing the probability \mathcal{P} of observing a microscopic trajectory γ to the probability of its reverse $\tilde{\gamma}$ occurring in a distinct thermodynamic process:

$$\Delta S_{\text{tot}}[\gamma] = \ln \frac{\mathcal{P}[\gamma]}{\tilde{\mathcal{P}}[\tilde{\gamma}]}, \quad (2)$$

$$\Delta S_{\text{na}}[\gamma] = \ln \frac{\mathcal{P}[\gamma]}{\tilde{\mathcal{P}}^+[\tilde{\gamma}]}, \quad \Delta S_{\text{a}}[\gamma] = \ln \frac{\mathcal{P}[\gamma]}{\mathcal{P}^+[\gamma]}, \quad (3)$$

where the probability densities $\tilde{\mathcal{P}}$ and \mathcal{P}^+ correspond to different notions of time reversal whose definitions will be elaborated later. The advantage of representing these entropy productions as ratios of trajectory probabilities is that it immediately implies that they each satisfy an integral fluctuation theorem, and each are positive on average [2]: $\Delta S_{\text{tot}} = \langle \Delta S_{\text{tot}} \rangle \geq 0$, $\Delta S_{\text{na}} = \langle \Delta S_{\text{na}} \rangle \geq 0$ and $\Delta S_{\text{a}} = \langle \Delta S_{\text{a}} \rangle \geq 0$, where the angle brackets denote an average over all trajectories.

Since the discovery of the fluctuation theorems, extending them, and subsequently (1), to a quantum setting has been an active pursuit [7, 8]. Still, a decomposition akin to (1) for quantum thermodynamics is lacking. In this paper, we develop such a decomposition. Our approach is to take (2) and (3) as defining equations for the various entropy productions. However, adapting them to a quantum setting requires a consistent interpretation of a trajectory for an open quantum system. The trajectories we analyze here are the individual realizations of a quantum Markov jump process of a finite-dimensional open quantum system. In particular, we model the evolution of an open quantum system by employing the repeated interaction method originally proposed in quantum optics [9–12]. Within this formalism the effect of an infinite environment is modeled as a rapid sequence of interactions with a series of copies of one small quantum system. A prototypical example from quantum optics is a series of two-level atoms that by rapidly passing through a superconducting cavity can act as a thermal reservoir for the confined electromagnetic radiation [13]. After each copy interacts, we measure it, allowing us to indirectly monitor the evolution of our system of interest. Roughly speaking, this is the least intrusive method of observation, since the measurement, being made after the interaction, cannot affect the system due to causality. Moreover, by monitoring the environment we have direct access to the energy that flows into the surroundings as heat. This allows us the capability to not only analyze entropy production, but also the energy balance between work, heat and internal energy in line with the quantum stochastic thermodynamics introduced by one of us in [14].

Derivations of fluctuation theorems based on monitoring the environment, as we do here, were realized previously by Dereziński, De Roeck and Maes for heat currents in steady state [15, 16]; as well as by Crooks for the work done on a weakly coupled Markovian open quantum system isothermally driven away from equilibrium [17]; and most recently by Hekking and Pekola [18] for the work dissipated in an isothermally driven two-level system. The novelty of the present endeavor is to explicitly address driven systems in conjunction with dissipative currents. Moreover, by carefully modeling the system–environment interaction in the Markovian limit, we are led to a robust formula for environment entropy production ((30) below) that applies not only to equilibrium environments but also to more general surroundings—such as the coherent thermal reservoirs that can induce lasing without inversion [19].

We begin our analysis in section 2 by introducing our system of interest and defining notation. Then in sections 3 and 4 conditions are introduced and analyzed for the total entropy production to satisfy a detailed fluctuation theorem within the repeated interaction framework

in general and specifically for quantum Markov jump processes. Nonadiabatic and adiabatic entropy production are discussed for quantum jump processes in section 5, before concluding in section 7.

2. Setup

2.1. Repeated interaction framework

We have in mind a finite-dimensional quantum system whose density matrix at time t we denote ρ_t . Its time-reversal invariant Hamiltonian $H(\lambda)$ is parameterized by a collection of externally controlled parameters λ , which we vary with time to do work on the system. The surroundings are modeled by coupling the system to a rapid sequence of N copies of a finite-dimensional quantum system with Hilbert space \mathcal{H}_E and time-reversal invariant Hamiltonian $H_E = \sum_l \varepsilon_l \Pi_l$, where $\varepsilon_l \neq \varepsilon_k$ for $l \neq k$ and each Π_l projects onto the associated energy eigenspace \mathcal{H}_l . To be concise, we will call each such copy an *environment*. Prior to interacting with the system, each environment is with probability p_l in a known density matrix r_l whose support is confined to \mathcal{H}_l . For example, in an equilibrium environment at inverse temperature β each state occurs with Boltzmann weight, so each $r_l = \Pi_l/d_l$ is diagonal in the energy basis with d_l the dimension of the l energy eigenspace, and $p_l \propto d_l e^{-\beta \varepsilon_l}$. Each copy interacts with the system for a time τ through the interaction

$$V(\lambda) = h \sum_{k \neq l} S_{kl}(\lambda) \otimes R_{kl}, \quad (4)$$

which is mediated by environment operators R_{kl} ($k \neq l$) that map vectors from one energy eigenspace \mathcal{H}_l to another \mathcal{H}_k and that we require to obey the symmetry $R_{kl} = R_{lk}^\dagger$. Here, h is the coupling strength, and $S_{kl}(\lambda)$ are parameter-dependent system operators that verify $S_{kl} = S_{lk}^\dagger$, since V must be Hermitian. After the interaction, we make an ideal projective measurement to determine whether the environment remained in \mathcal{H}_l or transitioned to another eigenspace \mathcal{H}_k . By recording transitions between energy subspaces, we track the total amount of energy that flows into the surroundings as heat. This is a minimal requirement to be able to formulate a first-law-like energy balance equation for a quantum stochastic thermodynamics [14].

The time-reversal invariance of $H(\lambda)$, H_E , and V assumed above is imposed by requiring that they each commute with the time-reversal operator Θ , which is an anti-unitary operator that satisfies $\Theta^2 = I$. This further implies that the energy eigenstates of $H(\lambda)$ and H_E do not change under the action of Θ and $[\Theta, R_{kl}] = 0$.

2.2. Quantum thermodynamic process

Within the framework of stochastic thermodynamics, the entropy production is connected to the ratio of the probabilities to observe different trajectories along distinct thermodynamic processes, as can be seen in (2) and (3). Therefore, in order to discern the quantum entropy production, we first review the class of quantum thermodynamic processes appropriate for the repeated interaction setup, allowing for driving by an external agent and possibly nonequilibrium environments. This class of processes is inspired by the cavity quantum electrodynamics experiments proposed in [9, 13, 20].

The *forward* process begins by preparing the initial ensemble diagonal in the eigenbasis of an observable A with nondegenerate eigenvalues a , $\rho_A \equiv \sum_a P_a |a\rangle\langle a|$. After randomly

selecting a system from this ensemble, we measure A to confirm the initial state $|a\rangle$. Then from $t = 0$ to $T = N\tau$, we drive the system with protocol $\Lambda = \{\lambda_t\}_{t=0}^T$, while it interacts with the sequence of environments. During the k th step ($k = 1, \dots, N$) from $t = (k-1)\tau$ to $k\tau$, an environment initially in the \mathcal{H}_{i_k} subspace with density matrix r_{i_k} will end the interval in \mathcal{H}_{j_k} (where it may be $j_k = i_k$). Meanwhile, the system density matrix $\rho_{k-1} \equiv \rho_{(k-1)\tau}$ changes to ρ_k . This change in the system given that the transition $i_k \rightarrow j_k$ occurred is conveniently expressed in terms of the quantum operation

$$\mathcal{Q}_k = \mathcal{E}_{j_k i_k}(\rho_{k-1}) \equiv \text{Tr}_E[\Pi_{j_k} U_k(\rho_{k-1} \otimes p_{i_k} r_{i_k}) U_k^\dagger \Pi_{j_k}], \quad (5)$$

where U_k is the time-evolution operator coupling the system to the k th environment from $t = (k-1)\tau$ to $k\tau$. The quantum operation \mathcal{E} is a completely positive superoperator [21]. It does not preserve the trace of the system density matrix, and as such does not conserve probability. A point we emphasize with the notation by introducing the *unnormalized* density matrix \mathcal{Q}_k at time $t = k\tau$. The trace of $\mathcal{E}_{j_k i_k}$ (or \mathcal{Q}_k), instead, encodes the probability for observing the $i_k \rightarrow j_k$ transition, $P_{j_k i_k} = \text{Tr}_S[\mathcal{E}_{j_k i_k}(\rho_k)]$. Thus, the normalized post-interaction density matrix conditioned on the transition $i_k \rightarrow j_k$ is $\rho_k = \mathcal{Q}_k / P_{j_k i_k}$ ($= \mathcal{E}_{j_k i_k}(\rho_{k-1}) / P_{j_k i_k}$). At time $t = T$, the sequence of environments is stopped, and we measure another system observable B whose nondegenerate eigenvalues b occur with probability $P_b = \langle b | \rho_T | b \rangle$. The collection of measurement results we collect into a vector called the *measurement trajectory* $\gamma = \{a; i_1 \rightarrow j_1, \dots, i_N \rightarrow j_N; b\}$.

To obtain the probability of observing γ in the forward process, we first observe that the probability for each jump is the trace of $\mathcal{E}_{j_k i_k}$. Similarly for a sequence of transitions, we can obtain the probability of that sequence by repeated action of an \mathcal{E} for each transition. Thus, the probability to observe the sequence of transitions in γ is

$$\begin{aligned} \mathcal{P}[\gamma] &= \mathcal{P}[\gamma | a] P_a \\ &= \text{Tr}_S[|b\rangle \langle b| \mathcal{E}_{j_N i_N} \cdots \mathcal{E}_{j_1 i_1} |a\rangle \langle a|] P_a, \end{aligned} \quad (6)$$

where it is understood that each superoperator acts on all terms to the right.

Accompanying every forward process is a *reverse* process, where each action is carried out in the reverse order and time-reversed under the action of the time-reversal operator Θ . In particular, the initial density matrix is diagonal in the eigenbasis of $\tilde{B} = \Theta B \Theta^{-1}$, $|\tilde{b}\rangle = \Theta |b\rangle$, with entries P_b . After first measuring \tilde{B} at $t = 0$, we implement the reverse protocol $\tilde{\Lambda} = \{\lambda_{\tau-t}\}_{t=0}^T$ while the system interacts with a sequence of environments, each prepared in one of the time-reversed density matrices $\tilde{r}_j = \Theta r_j \Theta^{-1}$ with probability p_j . The accompanying quantum operation in the k th step is

$$\tilde{\mathcal{Q}}_k = \tilde{\mathcal{E}}_{i_k j_k}(\tilde{\rho}_{k-1}) \equiv \text{Tr}_E[\Pi_{i_k} \tilde{U}_k(\tilde{\rho}_{k-1} \otimes p_{j_k} \tilde{r}_{j_k}) \tilde{U}_k^\dagger \Pi_{i_k}]. \quad (7)$$

Here, \tilde{U}_k is the reverse time-evolution operator and is related to the forward time-evolution operator by *microscopic reversibility* [8]

$$\tilde{U}_k = \Theta U_{N-k+1}^\dagger \Theta^{-1}, \quad (8)$$

which may be verified by demonstrating that each side solves the same Schrödinger equation. The process is completed at $t = T$ by measuring $\tilde{A} = \Theta A \Theta^{-1}$. For every trajectory of the forward process γ there is a *conjugate reverse trajectory* in which we observe the reverse sequence, $\tilde{\gamma} = \{\tilde{b}; j_N \rightarrow i_N, \dots, j_1 \rightarrow i_1; \tilde{a}\}$, which occurs with probability

$$\begin{aligned} \tilde{\mathcal{P}}[\tilde{\gamma}] &= \tilde{\mathcal{P}}[\tilde{\gamma} | \tilde{b}] P_b \\ &= \text{Tr}_S[|\tilde{a}\rangle \langle \tilde{a}| \tilde{\mathcal{E}}_{i_1 j_1} \cdots \tilde{\mathcal{E}}_{i_N j_N} |\tilde{b}\rangle \langle \tilde{b}|] P_b. \end{aligned} \quad (9)$$

3. Total entropy production with repeated interactions

Having introduced the basic setup for modeling an open quantum systems with repeated interactions, we now investigate under what conditions we can use a detailed fluctuation theorem to identify the total entropy production. We see from (2) that for the detailed fluctuation theorem to hold, the ratio of $\mathcal{P}[\gamma]$ and $\tilde{\mathcal{P}}[\tilde{\gamma}]$ must depend only on γ , that is only on the sequence of transitions between energy eigenspaces in the environment and not on the particular state to state transitions. By inspection of (6) and (9), we have found two ways to accomplish this task. The first, which we address in this section, is for each environment to be proportional to an energy eigenspace projection operator. This scenario includes the case of one or many thermal reservoirs (possibly at different temperatures) and is commonly utilized in the derivations of the work fluctuation relations for unitary quantum dynamics [8]. The second option is to make the effect of each environment on the system small, which we develop in section 4.

To understand how an environment proportional to an energy eigenspace projection operator leads to a detailed fluctuation theorem for the total entropy production, we expand the conditional probability to observe a trajectory γ given the initial state $|a\rangle$ in (6) using the definition of \mathcal{E} in (5):

$$\mathcal{P}[\gamma|a] = \text{Tr}_{SE} [|b\rangle\langle b| (\Pi_{j_N} U_N \cdots \Pi_{j_1} U_1) |a\rangle\langle a| \bigotimes_{k=1}^N p_{i_k} r_{i_k} (U_1^\dagger \Pi_{j_1} \cdots U_N^\dagger \Pi_{j_N})]. \quad (10)$$

When $r_i = \Pi_i/d_i$, this expression may be simplified by evaluating the trace in the energy eigenbasis of the environment. Denoting by $\{|\alpha_{i_k}\rangle\}$ the energy eigenbasis of each eigenspace \mathcal{H}_{i_k} , we have

$$\mathcal{P}[\gamma|a] = \sum_{\alpha_{i_1}, \alpha_{j_1}, \dots, \alpha_{i_N}, \alpha_{j_N}} |\langle b, \alpha_{j_N}, \dots, \alpha_{j_1} | U_N \cdots U_1 | a, \alpha_{i_N}, \dots, \alpha_{i_1} \rangle|^2 \frac{p_{i_N}}{d_{i_N}} \cdots \frac{p_{i_1}}{d_{i_1}}, \quad (11)$$

recalling that $[U_k, \Pi_{j_l}] = 0$ for $k \neq l$, since they act on different environments. Similarly, for the reverse process we have

$$\mathcal{P}[\tilde{\gamma}|\tilde{b}] = \sum_{\alpha_{i_1}, \alpha_{j_1}, \dots, \alpha_{i_N}, \alpha_{j_N}} |\langle \tilde{b}, \alpha_{i_1}, \dots, \alpha_{i_N} | \tilde{U}_N \cdots \tilde{U}_1 | \tilde{b}, \alpha_{j_1}, \dots, \alpha_{j_N} \rangle|^2 \frac{p_{j_1}}{d_{j_1}} \cdots \frac{p_{j_N}}{d_{j_N}} \quad (12)$$

$$= \sum_{\alpha_{i_1}, \alpha_{j_1}, \dots, \alpha_{i_N}, \alpha_{j_N}} |\langle b, \alpha_{j_N}, \dots, \alpha_{j_1} | U_N \cdots U_1 | a, \alpha_{i_N}, \dots, \alpha_{i_1} \rangle|^2 \frac{p_{j_1}}{d_{j_1}} \cdots \frac{p_{j_N}}{d_{j_N}}, \quad (13)$$

where the second line follows from the anti-unitarity of Θ , the time-reversal invariance of H_E ($\Theta|\alpha_i\rangle = |\alpha_i\rangle$) and the microscopic reversibility condition in (8).

Now we see that the ratio of $\mathcal{P}[\gamma|a]$ and $\tilde{\mathcal{P}}[\tilde{\gamma}|\tilde{b}]$ only depends on the sequence of environment jumps, $i_k \rightarrow j_k$, as the dependence on the $\{|\alpha_{i_k}\rangle\}$ cancels. Thus, we can identify entropy production in line with (2) through the relation

$$\Delta s_{\text{tot}}[\gamma] = \Delta s[\gamma] + \Delta s_{\text{env}}[\gamma] = \ln \frac{\mathcal{P}[\gamma|a] P_a}{\tilde{\mathcal{P}}[\tilde{\gamma}|\tilde{b}] P_b} \quad (14)$$

with environment entropy production

$$\Delta s_{\text{env}}[\gamma] = \ln \frac{\mathcal{P}[\gamma|a]}{\tilde{\mathcal{P}}[\tilde{\gamma}|\tilde{b}]} = \sum_{k=1}^N \ln \left(\frac{p_{i_k} d_{j_k}}{d_{i_k} p_{j_k}} \right), \quad (15)$$

and system entropy change

$$\Delta s[\gamma] = -\ln P_b + \ln P_a. \quad (16)$$

Notice that these results do not depend on the form of the interaction V in (4), and therefore apply to any interaction.

We substantiate our identifications of Δs_{env} and Δs in (15) and (16) as follows. For an equilibrium environment, $p_j \propto d_j e^{-\beta \varepsilon_j}$ and the environment entropy production in (15) is related to the total heat flow into the environment $q[\gamma] = \sum_k (\varepsilon_{j_k} - \varepsilon_{i_k})$ as

$$\Delta s_{\text{env}}^{\text{eq}}[\gamma] = \sum_{k=1}^N \beta (\varepsilon_{j_k} - \varepsilon_{i_k}) = \beta q[\gamma], \quad (17)$$

as expected for a thermal reservoir. We call (16) the system's trajectory entropy change [14], because upon averaging over all trajectories, we find that $\Delta S = \langle \Delta s \rangle = S(\rho_T) - S(\rho_0)$ is simply the change in the von Neumann entropy $S(\rho) = -\text{Tr}_S[\rho \ln \rho]$ of the system density matrix during the forward process from $\rho_0 = \sum_a P_a |a\rangle\langle a|$ to $\rho_T = \sum_b P_b |b\rangle\langle b|$. (Recall that the measurements of A and B force the system density matrix to be diagonal in the eigenbases of A and B at the beginning and end of the forward process.)

This result, however, is just a special case of the two-point measurement scheme commonly utilized in the derivation of quantum fluctuation relations with unitary dynamics for work [8] and currents [7, 22]. In this framework, measurements of the system and surroundings are only made at the beginning of the process, at time $t = 0$, and at the end when $t = T$. For example, work fluctuations in open quantum systems can be identified by measuring the initial and final energies of the system and its surroundings [8]. The change in system energy is the change in internal energy ΔU ; the change in energy of the surroundings can be equated with the heat flow into the system Q ; their difference is the work $W = \Delta U - Q$.

The predictions of this section fit into this two-point measurement scheme, because (11) naturally can be interpreted as a two-point measurement. Initially the system observable A is measured along with the energy of every environment (the surroundings). Then after a unitary evolution the observable B is measured with another measurement of the energy of every environment. Thus it makes no difference whether we measure all the environments at once upon completing the process, or measure them continually as the process evolves.

4. Entropy production for quantum jump trajectories

An alternative approach to investigating entropy production through detailed fluctuation theorems, even in the case of nonequilibrium environments, is to tune the interaction between the system and the environment so that each environment only affects the system a little. One possibility is to make the coupling strength small, an approach often called the weak-coupling limit. This approach we will wait to comment on till the conclusion in section 7. Here, we consider another scenario typically encountered in quantum optics as a means to model continuous measurement [9, 20, 23], and analyzed rigorously by Nechita and Pellegrini in [24]. To make the environment's effect small, we take the interaction time to be short, $\hbar\tau \ll 1$. As a result, many environments interact with the system before it changes appreciably. Analyzing the evolution on this longer time-scale during which the system changes, leads to an effective coarse-grained dynamics described by a quantum Markov process. Despite the additional complications arising from passing to this limit, we find new possibilities for the

types of environments we can consider and furthermore are able to develop trajectory-dependent definitions of the nonadiabatic and adiabatic entropy productions.

4.1. Effective dynamics and the stochastic master equation

When the interaction time is short, it is natural to use an effective dynamics on a coarse-grained time scale that captures the effect of the rapid sequence of environments. To achieve this limit, we take τ small with a scaled coupling $h = \sqrt{g/\tau}$. We then find in appendix A that on a coarse-grained time scale, with an infinitesimal increment $dt \gg \tau$ long enough that many environments interact with the system, the dynamics are well described as a Poisson process with jumps due to rare transitions in the environment. This limit requires that we further assume that the variation in the external parameters is not too fast, $\dot{\lambda}_t dt \ll 1$, and that the bare evolution generated by the system Hamiltonian $H(\lambda_t)$ over a small dt interval is small.

The chance of observing a jump in the environment in any small dt is very small. When we do observe a jump, say at time t from $\mathcal{H}_i \rightarrow \mathcal{H}_j$, the system density matrix ρ_t changes under the action of the jump operation

$$\rho_{t+dt} = \mathcal{J}_{ji}(\rho_t) \equiv L_{ji}(\lambda_t)\rho_t L_{ji}^\dagger(\lambda_t) dt, \quad (18)$$

where the *jump (or Lindblad) operators* are

$$L_{kl}(\lambda) = \sqrt{gp_l \langle R_{kl}^\dagger R_{kl} \rangle_l} S_{kl}(\lambda) \quad (19)$$

with jump (or decay) rate $g = h^2\tau$ and $\langle R_{kl}^\dagger R_{kl} \rangle_l = \text{Tr}_E[R_{kl}^\dagger R_{kl} r_l]$ is the environment correlation function. The trace of the jump operation \mathcal{J}_{kl} (or ρ_{t+dt}) is the probability to observe the transition $P_{kl} = \text{Tr}_S[\mathcal{J}_{kl}(\rho)] \sim dt$, which is of order dt demonstrating the anticipated Poisson statistics. In between the jumps, say from time s to t , the evolution is smooth and given by

$$\rho_t = \mathcal{U}_{t,s}(\rho_s) \equiv U_{\text{eff}}(t, s)\rho_s U_{\text{eff}}^\dagger(t, s), \quad (20)$$

where U_{eff} is a non-unitary *effective time evolution operator* defined as the solution of (with $\hbar = 1$)

$$\frac{\partial}{\partial t} U_{\text{eff}}(t, s) = -iH_{\text{eff}}(\lambda_t)U_{\text{eff}}(t, s) \quad (21)$$

with initial condition $U_{\text{eff}}(s, s) = I$, where I is the identity operator. Here,

$$H_{\text{eff}}(\lambda) = H(\lambda) - \frac{i}{2} \sum_{kl} L_{kl}^\dagger(\lambda)L_{kl}(\lambda) \quad (22)$$

is a non-Hermitian *effective Hamiltonian*. The operation \mathcal{U} encodes the distribution of wait-times between jumps: the probability to wait from time s to t in state ρ without observing a jump is $P_{\text{wait}}(t, s) = \text{Tr}_S[\mathcal{U}_{t,s}\rho]$.

The system evolution conditioned on the environmental changes is a stochastic process, where the smooth evolution \mathcal{U} is punctuated by random jumps due to \mathcal{J} that occur with Poisson statistics. A useful alternative way to formulate this observation is in terms of a stochastic master equation for the conditioned system density matrix [25]. Here the Poisson jump statistics are incorporated by introducing a collection of Poisson increments dN_t^{kl} , one for each type of jump between energy subspaces that can be observed. These increments are 1 when a jump is observed between $(t, t + dt)$ and 0 otherwise. Formally they are characterized by the relation

$(dN_t^{kl})^2 = dN_t^{kl}$ and their classical expectation

$$E[dN_t^{kl}] = \text{Tr}_S[L_{kl}^\dagger(\lambda_t)L_{kl}(\lambda_t)\rho_t] dt. \quad (23)$$

In terms of these stochastic increments the evolution captured by (18) and (20) can be given in a compact form as the Itô stochastic differential equation for the stochastic increment of the unnormalized density matrix $d\varrho_t = \varrho_{t+dt} - \varrho_t$ [25]

$$d\varrho_t = -i(H_{\text{eff}}(\lambda_t)\varrho_t - \varrho_t H_{\text{eff}}^\dagger(\lambda_t)) dt + \sum_{kl} dN_t^{kl}(L_{kl}(\lambda_t)\varrho_t L_{kl}^\dagger(\lambda_t) - \varrho_t). \quad (24)$$

This equation describes the conditioned behavior of the density matrix. The (unconditioned) average behavior of the normalized density matrix $\rho_t = \varrho_t/\text{Tr}_S[\varrho_t]$ follows the Lindblad master equation [21]

$$\frac{\partial}{\partial t}\rho_t = -i[H(\lambda_t), \rho_t] + \sum_{kl} \mathcal{D}[L_{kl}(\lambda_t)]\rho_t \equiv \mathcal{L}_{\lambda_t}\rho_t, \quad (25)$$

where $\mathcal{D}[c]\rho = c\rho c^\dagger - \frac{1}{2}c^\dagger c\rho - \frac{1}{2}\rho c^\dagger c$. The dynamics generated by (25) is a quantum Markov semigroup and is the closest analogue of a classical Markov process. It is worth noting that for a given master equation, such as (25), the representation in terms of jump operators L_{kl} is not unique: there exist different collections of jump operators (and H) that lead to the same evolution for ρ_t [21]. However, we have arrived at our representation using a particular microscopic model, singling out our representation with a particular measurement scheme. Different ways of monitoring are related to other representations [25].

In the reverse process, we have a similar situation. Jumps change the system by

$$\tilde{\mathcal{J}}_{ji}(\tilde{\rho}_t) = \tilde{L}_{ji}(\tilde{\lambda}_t)\tilde{\rho}_t\tilde{L}_{ji}^\dagger(\tilde{\lambda}_t) dt \quad (26)$$

with *reverse jump operators*

$$\tilde{L}_{kl}(\lambda) = \Theta L_{kl}(\lambda)\Theta^{-1} \quad (27)$$

derived in appendix A. Again, between jumps the dynamics are given by a *reverse effective time-evolution operator* $\tilde{U}_{\text{eff}}(t, s)$ defined as the solution of a Schrödinger equation, as in (21), except generated by the reverse effective non-Hermitian Hamiltonian $\tilde{H}_{\text{eff}}(\lambda) = \Theta H_{\text{eff}}^\dagger(\lambda)\Theta^{-1}$. As a result, we have the time-reversal symmetry

$$\tilde{U}_{\text{eff}}(t, s) = \Theta U_{\text{eff}}^\dagger(T - s, T - t)\Theta^{-1}. \quad (28)$$

4.2. Local detailed balance

At this point, we nearly have all the tools to demonstrate a detailed fluctuation theorem. The last ingredient is a time-reversal symmetry of the jump operators that can be deduced from their definitions in (19)

$$L_{kl}(\lambda) = L_{lk}^\dagger(\lambda)e^{\Delta s_{kl}/2}, \quad (29)$$

where we have identified the environment entropy production per jump

$$\Delta s_{kl} = \ln \frac{p_l \langle R_{kl}^\dagger R_{kl} \rangle_l}{p_k \langle R_{lk}^\dagger R_{lk} \rangle_k} = \ln \left(\frac{p_l}{d_l} \frac{d_k}{p_k} \right) + \ln \frac{\langle R_{kl}^\dagger R_{kl} \rangle_l d_l}{\langle R_{lk}^\dagger R_{lk} \rangle_k d_k}, \quad (30)$$

which differs from (15) by the addition of the second term depending on the environment correlation functions. For an equilibrium environment, as well as for a collection of distinct

equilibrium environments, $p_k \propto d_k e^{-\beta \varepsilon_k}$ and $r_k = \Pi_k/d_k$. As a result, the second term in (30) is zero, and we recover the expected result $\Delta s_{kl} = \beta(\varepsilon_k - \varepsilon_l)$ (cf (17)).

Equation (29) may be viewed as an operator version of the local detailed balance condition for classical Markov jump processes relating the probability of forward and reverse jumps to the entropy production in the environment. In light of this analogy, (29) is one of our main observations given the role that detailed balance plays in thermodynamically consistent descriptions of equilibrium and nonequilibrium processes. Equation (29), however, is valid for a wider variety of situations when $\langle R_{kl}^\dagger R_{kl} \rangle_l d_l \neq \langle R_{lk}^\dagger R_{lk} \rangle_k d_k$. In this case, there is an additional *thermodynamic force*

$$F_{kl} = \ln \frac{\langle R_{kl}^\dagger R_{kl} \rangle_l d_l}{\langle R_{lk}^\dagger R_{lk} \rangle_k d_k}, \quad (31)$$

driving the system out of equilibrium.

To clarify the origin of this force F , we briefly consider the simplest nontrivial example of an environment with two energy eigenspaces. The higher energy or excited subspace \mathcal{H}_e is one dimensional and spanned by $|e\rangle$. The second is a two-dimensional energy eigenspace \mathcal{H}_g spanned by the degenerate ground states $|g\rangle$ and $|g'\rangle$, with initial preparation

$$r_g = \begin{pmatrix} 0 & 0 & 0 \\ 0 & q & s \\ 0 & s^* & q' \end{pmatrix}, \quad (32)$$

expressed in the basis $\{|e\rangle, |g\rangle, |g'\rangle\}$ with $|q|^2 + |q'|^2 = 1$. To calculate F , we must determine the environment correlation functions $\langle R_{kl}^\dagger R_{kl} \rangle_l$. For transitions originating in the excited subspace, we must have $\langle R_{ge}^\dagger R_{ge} \rangle_e d_e = 1$, since \mathcal{H}_e is one dimensional. On the other hand, for transitions from the ground eigenspace to the excited state $|e\rangle$ we are free to choose the transition operator R_{eg} . The most general choice is

$$R_{eg} = \begin{pmatrix} 0 & a & b \\ 0 & 0 & 0 \\ 0 & 0 & 0 \end{pmatrix} \quad (33)$$

with a and b arbitrary complex numbers. A short algebraic calculation then reveals

$$\langle R_{eg}^\dagger R_{eg} \rangle_g d_g = 2(q|a|^2 + q'|b|^2 + a^* b s^* + a b^* s), \quad (34)$$

which upon substitution into (31) leads to a force

$$F_{eg} = -F_{ge} = \ln[2(q|a|^2 + q'|b|^2 + a^* b s^* + a b^* s)]. \quad (35)$$

The force is nonzero when there is coherence in the environment in the energy basis ($s \neq 0$). A nonzero force also arises even without coherence ($s = 0$), when $q|a|^2 + q'|b|^2 \neq 1/2$, which depends on the environment *and* the interaction. In one of our illustrative examples in section 6, we will further explore F within the lasing-without-inversion setting where each environment has some coherence in the energy basis.

4.3. Total entropy production

In the description of the process given by the stochastic dynamics, the trajectory γ can be reduced to the collection of jumps $i_k \rightarrow j_k$ and the times t_k at which they occur: $\gamma = \{a; t_1, i_1 \rightarrow j_1; \dots; t_K, i_K \rightarrow j_K; b\}$. This is a welcome simplification, because only when there is a change

in the environment is there heat flow or entropy production. As before, the quantum operations in (18) and (20) encode the probabilities to observe such a trajectory (see (6)),

$$\begin{aligned} \mathcal{P}[\gamma|a] &= \text{Tr}_S[|b\rangle\langle b|\mathcal{U}_{T,t_K} \cdots \mathcal{J}_{j_1 i_1} \mathcal{U}_{t_1,0}|a\rangle\langle a|] \\ &= |\langle b|U_{\text{eff}}(T, t_K) \cdots L_{j_1 i_1}(\lambda_{t_1})U_{\text{eff}}(t_1, 0)|a\rangle|^2 dt_1 \cdots dt_K. \end{aligned} \quad (36)$$

For any trajectory of the forward process $\gamma = \{a; t_1, i_1 \rightarrow j_1; \dots; t_K, i_K \rightarrow j_K; b\}$ we have a conjugate reverse trajectory $\tilde{\gamma} = \{b; T - t_K, j_K \rightarrow i_K; \dots; T - t_1, j_1 \rightarrow i_1; \tilde{a}\}$ that occurs in the reverse process with probability

$$\begin{aligned} \tilde{\mathcal{P}}[\tilde{\gamma}|\tilde{b}] &= \text{Tr}_S[|\tilde{a}\rangle\langle \tilde{a}|\tilde{\mathcal{U}}_{T,T-t_1} \cdots \tilde{\mathcal{J}}_{i_K j_K} \tilde{\mathcal{U}}_{T-t_K,0}|\tilde{b}\rangle\langle \tilde{b}|] \\ &= |\langle \tilde{a}|\tilde{U}_{\text{eff}}(T, T - t_1) \cdots \tilde{L}_{i_K j_K}(\tilde{\lambda}_{T-t_K})\tilde{U}_{\text{eff}}(T - t_K, 0)|\tilde{b}\rangle|^2 dt_1 \cdots dt_K. \end{aligned} \quad (37)$$

It is now straightforward to arrive at a detailed fluctuation theorem by comparing the definitions of \mathcal{P} and $\tilde{\mathcal{P}}$ in (36) and (37) after substituting in the definition of \tilde{L}_{ji} in (27) and the time-reversal symmetries in (28) and (29):

$$\frac{\mathcal{P}[\gamma|a]}{\tilde{\mathcal{P}}[\tilde{\gamma}|\tilde{b}]} = e^{\Delta s_{\text{env}}[\gamma]} \quad (38)$$

with trajectory environment entropy change

$$\Delta s_{\text{env}}[\gamma] = \sum_{k=1}^K \Delta s_{j_k i_k}. \quad (39)$$

The total entropy production then follows as

$$\Delta s_{\text{tot}}[\gamma] = \Delta s[\gamma] + \Delta s_{\text{env}}[\gamma] = \ln \frac{\mathcal{P}[\gamma|a]P_a}{\tilde{\mathcal{P}}[\tilde{\gamma}|\tilde{b}]P_b}, \quad (40)$$

which extends [14].

Again, we have seen that a detailed fluctuation theorem for the total entropy production has a consistent interpretation. When the environments are prepared with $r_l = \Pi_l/d_l$, this prediction is a special case of the setup in section 3. The advantage comes from the possible addition of the quantum thermodynamic force F_{kl} in (31), and in the following section where we provide consistent definitions of the nonadiabatic and adiabatic entropy productions that would not be possible within the framework of finite-time interactions in section 3.

5. Nonadiabatic and adiabatic entropy productions

The effective stochastic description of the previous section affords us the further possibility to address detailed fluctuation theorems on the level of trajectories for adiabatic and nonadiabatic entropy productions. Like the total entropy production, ΔS_a and ΔS_{na} can be determined from ratios of path probabilities. Here, one compares the system's evolution to its dual: a time-reversed dynamics where, roughly speaking, all the dissipative stationary currents flow in reverse. Therefore, in this section we first review some properties of the dual of a quantum Markov process in section 5.1 before identifying quantum versions of the nonadiabatic and adiabatic entropy productions in section 5.2.

5.1. Dual process

The dual process is defined only in the absence of driving, which we call the *frozen* dynamics. In this case, the (unconditioned) system density matrix evolves according to a master equation $\partial_t \rho_t = \mathcal{L}_\lambda \rho_t$ (25) generated by the superoperator \mathcal{L}_λ , where λ has a fixed value. We further assume that this equation has a unique, positive-definite, stationary density matrix π_λ , given as the solution of $\mathcal{L}_\lambda \pi_\lambda = 0$.

With the definition of the frozen dynamics in hand, the dual dynamics for each fixed λ is the dynamics for which the stationary state probability of observing a reverse trajectory $\tilde{\gamma}$, $\mathcal{P}_{\text{st}}^+[\tilde{\gamma}]$, is the same as observing the conjugate trajectory γ in the original process: $\mathcal{P}_{\text{st}}^+[\tilde{\gamma}] = \mathcal{P}_{\text{st}}[\gamma]$ [17]. The existence of a dual that is also a quantum Markov semigroup—a dynamics whose averaged evolution is described by a Lindblad master equation, as in (25)—is nontrivial. However, we are assured of its existence, since we assume a finite-dimensional system and a unique, positive-definite, stationary density matrix π_λ [26].

Like the original process the dual process is characterized by a collection of *dual jump operators* $L_{kl}^+(\lambda)$ and a *dual effective time-evolution operator* $U_{\text{eff}}^+(t, s)$. By comparing $\mathcal{P}_{\text{st}}^+[\tilde{\gamma}]$ and $\mathcal{P}_{\text{st}}[\gamma]$, we demonstrate in appendix B that the dual operators are

$$L_{kl}^+(\lambda) = \Theta \pi_\lambda^{1/2} L_{lk}^\dagger(\lambda) \pi_\lambda^{-1/2} \Theta^{-1} \quad (41)$$

and

$$U_{\text{eff}}^+(t, s) = \Theta \pi_\lambda^{1/2} U_{\text{eff}}^\dagger(T - s, T - t) \pi_\lambda^{-1/2} \Theta^{-1}, \quad (42)$$

which agrees with [26–28]. We can simplify these expressions by recalling that the representation of the dynamics in terms of jump operators is not unique (see the discussion following (25)). There is a special representation called the *privileged representation* in which the dual operators take a particularly simple form [26]. This *privileged representation* with respect to π_λ is defined by the properties

$$\pi_\lambda L_{kl}(\lambda) = \varpi_{kl}(\lambda) L_{kl}(\lambda) \pi_\lambda, \quad (43)$$

$$[H(\lambda), \pi_\lambda] = \left[\sum_{kl} L_{kl}^\dagger(\lambda) L_{kl}(\lambda), \pi_\lambda \right] = 0 \quad (44)$$

for some $\varpi_{kl}(\lambda)$, which verify $\varpi_{kl} = \varpi_{lk}^{-1}$. These ϖ_{kl} are ratios of the eigenvalues of π_λ : in particular, if we expand $\pi_\lambda = \sum_n p_n^{\text{st}} |e_n\rangle \langle e_n|$ in its diagonal basis, then $\varpi_{kl}(\lambda) = p_n^{\text{st}}/p_m^{\text{st}}$ for all states $|e_n\rangle$ and $|e_m\rangle$ connected by L_{kl} [26]. In other words, each L_{kl} only connects pairs of states whose stationary state probabilities have the same ratio. Furthermore, the conditions in (44) imply that the stationary density matrix π_λ is diagonal in the system energy eigenbasis.

In the privileged representation, assuming that the jump operators are time-reversal invariant $\Theta L_{kl} \Theta^{-1} = L_{kl}$, the dual jump operators are simply proportional to the original jump operators

$$L_{kl}^+(\lambda) = \varpi_{kl}^{1/2}(\lambda) L_{lk}^\dagger(\lambda), \quad (45)$$

which follows from substituting (43) into (41). Furthermore, we show in appendix B that (42) for U_{eff}^+ simplifies to

$$U_{\text{eff}}^+(t, s) = U_{\text{eff}}(t, s), \quad (46)$$

by verifying that both sides solve the same differential equation. Equation (45) is reminiscent of the classical definition of a dual Markov process in terms of ratios of stationary state probabilities. Furthermore, (46) is the quantum equivalent of the property that the wait-time distributions for a classical Markov process and its dual are equal. In the following, we assume that the dynamics are in the privileged representation. This may seem to be a restriction; however, in the examples analyzed in section 6 the dynamics naturally take this form, pointing to the possibility that for a quantum thermodynamic process this is generic.

5.2. Nonadiabatic and adiabatic entropy productions

Esposito and Van den Broeck [2] have shown that the adiabatic and nonadiabatic entropy productions can be identified as ratios of trajectory probabilities as in (3). We now use that connection to define the quantum analogues for quantum jump trajectories as ratios of $\mathcal{P}[\gamma]$ to the probabilities of observing γ in the dual dynamics, $\mathcal{P}^+[\gamma]$, or $\tilde{\gamma}$ in the dual dynamics during the reverse process, $\tilde{\mathcal{P}}^+[\tilde{\gamma}]$:

$$\Delta s_{\text{na}}[\gamma] = \ln \frac{\mathcal{P}[\gamma]}{\tilde{\mathcal{P}}^+[\tilde{\gamma}]}, \quad \Delta s_{\text{a}}[\gamma] = \ln \frac{\mathcal{P}[\gamma]}{\mathcal{P}^+[\gamma]}. \quad (47)$$

Roughly speaking, Δs_{a} and Δs_{na} are two measures of how distinguishable the system's evolution is from its dual. The nonadiabatic entropy production Δs_{na} is due to the breaking of time reversal by the external driving; whereas, the adiabatic contribution Δs_{a} is due to nonequilibrium boundary conditions.

Useful formulae for Δs_{a} and Δs_{na} are obtained by exploiting the symmetry in (45) and

$$\tilde{L}_{kl}^+(\lambda) = \varpi_{kl}^{1/2}(\lambda) \Theta L_{lk}^\dagger(\lambda) \Theta^{-1}, \quad (48)$$

for the dual operators of the reverse process, which may be deduced by combining (27) with the definition of L_{kj}^+ in (45). Substituting this symmetry, (45), (46) and $\varpi_{kl} = \varpi_{lk}^{-1}$ into (47), we find that

$$\Delta s_{\text{na}}[\gamma] = \Delta s[\gamma] + \sum_{k=1}^K \ln \varpi_{j_k i_k}(\lambda_{t_k}), \quad (49)$$

$$\Delta s_{\text{a}}[\gamma] = \Delta s_{\text{env}}[\gamma] - \sum_{k=1}^K \ln \varpi_{j_k i_k}(\lambda_{t_k}), \quad (50)$$

reminiscent of their classical analogues: the ϖ_{ji} have the form of ratios of stationary state probabilities, as would appear in the classical expressions. Continuing the classical analogy, we also identify the excess entropy production [29]

$$\Delta s_{\text{ex}}[\gamma] = \sum_{k=1}^K \ln \varpi_{j_k i_k}(\lambda_{t_k}). \quad (51)$$

6. Illustrations

In this section we illustrate the nonadiabatic and adiabatic entropy productions. Our first example is a three-level atom coupled to a coherent reservoir, inducing a nonzero quantum thermodynamic force (31). Our second example is a driven harmonic oscillator coupled to two different thermal reservoirs at inverse temperatures β and β' .

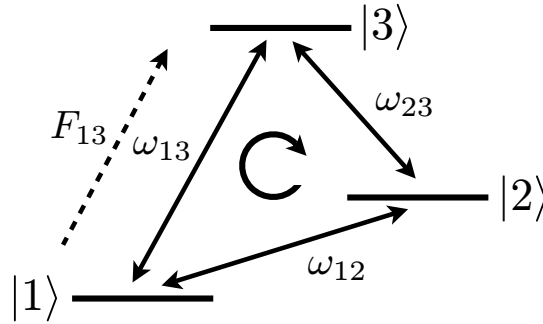


Figure 1. Illustration of the three-state atom with states $|1\rangle$, $|2\rangle$ and $|3\rangle$ and transition energies ω_{12} , ω_{23} and ω_{13} . A quantum thermodynamic force F_{13} due to coherence in the environments coupling states $|1\rangle$ and $|3\rangle$ drives transitions (dotted arrow), generating a nonzero, clockwise current (circular arrow).

6.1. Coherent thermal reservoir

To demonstrate how a nonzero quantum thermodynamic force F (31) can appear, we analyze a three-level atom coupled to a coherent thermal reservoir. Thermodynamic consequences of adding coherence to a thermal reservoir were first discussed by Scully *et al* [19, 30, 31] in the context of a photo-Carnot engine. Remarkably, the additional coherence was found to increase the overall efficiency of the engine. Similar increases in efficiency due to coherence were observed by Dillenschneider and Lutz for a sequence of entangled environments [32]. Each of these studies point to the surprising effects quantum coherence in the surroundings have on the thermodynamics of a system.

Here, we have in mind a three-level atom with states $|1\rangle$, $|2\rangle$ and $|3\rangle$ and transition energies $\omega_{mn} > 0$ ($m, n = 1, 2, 3$), as depicted in figure 1. In this example, we will assume that the external parameters are fixed, so that we can focus on the effect of F . The surroundings are implemented by coupling each transition to a rapid sequence of atoms, which play the role of our environments. The transitions between $|1\rangle \leftrightarrow |2\rangle$ and $|2\rangle \leftrightarrow |3\rangle$ are mediated by two-level atoms resonantly coupled. For example, in the $|1\rangle \leftrightarrow |2\rangle$ transition, the two-level atoms have states $|e\rangle$ and $|g\rangle$, energy difference ω_{12} and are coupled through the interaction

$$v_{12} = h(|2\rangle\langle 1|\sigma + |1\rangle\langle 2|\sigma^\dagger), \quad (52)$$

where $\sigma = |g\rangle\langle e|$. Each atom is initially prepared in equilibrium at inverse temperature β with $p_e/p_g = e^{-\beta\omega_{12}}$. The $|2\rangle \leftrightarrow |3\rangle$ transition is implemented in exactly the same manner with a different stream of two-level atoms at equilibrium at inverse temperature β with transition energy ω_{23} . On the other hand, the $|1\rangle \leftrightarrow |3\rangle$ transitions are mediated by a stream of three-level atoms in the Λ -configuration, depicted in figure 2, with excited state $|e\rangle$ and degenerate ground states $|g\rangle$ and $|g'\rangle$. We set the interaction (4) for these transitions such that the states $|g\rangle$ and $|g'\rangle$ of the bath are both mapped to $|e\rangle$ when the system jumps from $|3\rangle \rightarrow |1\rangle$, whereas $|e\rangle$ jumps to the linear combination $(|g\rangle + |g'\rangle)/\sqrt{2}$ in a $|1\rangle \rightarrow |3\rangle$ transition. Moreover, these three-level atoms are prepared in a coherent thermal state at inverse temperature β : the two energy eigenspaces \mathcal{H}_e and \mathcal{H}_g each occur according to the Boltzmann weight $p_e/p_g = e^{-\beta\omega_{13}}/2$. However, the density matrix in the \mathcal{H}_g subspace spanned by $|g\rangle$ and $|g'\rangle$ is prepared with off-diagonal elements in the energy basis according to the density matrix $r_g = \chi$. The off-diagonal elements $\chi_{gg'} = \chi_{g'g}^*$ cause interference when the environment atom jumps from \mathcal{H}_g

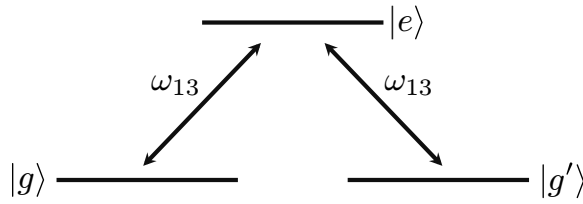


Figure 2. Illustration of the three-state atoms in a Λ -configuration that mediate the $|1\rangle \leftrightarrow |3\rangle$ transition through a resonant coupling. Coherence between the degenerate ground states $|g\rangle$ and $|g'\rangle$ reduces the transition rate to the excited state $|e\rangle$ leading to the appearance of the thermodynamic force F_{13} .

to \mathcal{H}_e , slowing the rate of transitions from $|3\rangle \rightarrow |1\rangle$. This leads to a relative enhancement in the rate of $|1\rangle \rightarrow |3\rangle$ transitions accompanied by a nonequilibrium current flowing between the different states of our three-level atom.

Carrying out the program outlined in section 4, we find that there are six jump operators L_{kl} connecting the different states $|l\rangle$ to $|k\rangle$ ($k, l = 1, 2, 3$). Here, we label the jump operators by state transitions instead of environment transitions, because each environment transition naturally corresponds to only one state transition. The six jump operators satisfy local detailed balance (29):

$$L_{13} = e^{(\beta\omega_{13} + F_{13})/2} L_{31}^\dagger, \quad (53)$$

$$L_{23} = e^{\beta\omega_{23}/2} L_{32}^\dagger, \quad (54)$$

$$L_{12} = e^{\beta\omega_{12}/2} L_{21}^\dagger, \quad (55)$$

where

$$F_{13} = \ln(1 + \chi_{gg'} + \chi_{g'g}) = \ln(1 + 2\text{Re } \chi_{gg'}). \quad (56)$$

Clearly, the force is only nonzero when there is some coherence in the energy eigenbasis ($\text{Re } \chi_{gg'} \neq 0$).

The nonzero value of F leads to entropy production as follows. Since the dynamics are autonomous—the external parameters are fixed—the system eventually relaxes to a steady state that is diagonal in the energy basis. At which point, the force F_{13} continually drives transitions $|1\rangle \rightarrow |3\rangle \rightarrow |2\rangle$ resulting in a nonzero stationary current J_{st} , running clockwise in figure 1. In this case, the average total entropy production rate takes the familiar form of force times flux, $\dot{S}_{\text{tot}} = F_{13} J_{\text{st}}$.

In their original analysis of the photo-Carnot engine, Scully *et al* [19] did not identify the thermodynamic force F . Instead they assigned a modified temperature T_{mod} to the coherent thermal reservoir that depended on the degree of coherence. This modified temperature was identifiable because they studied the photo-Carnot engine where the working substance is a single mode of the electromagnetic field, and when coupled to the coherent reservoir it relaxes to a Boltzmann distribution at the modified temperature T_{mod} . However, in our three-state atom model no such conclusion exists. The coherence maintains the system away from equilibrium leading to a constant entropy production.

6.2. Driven harmonic oscillator

In our second example, we present Δs_{na} and Δs_{a} for a driven quantum harmonic oscillator coupled to thermal reservoirs at different temperatures. The oscillator's Hamiltonian in terms of its position x , momentum p , frequency ω and mass m in units with $\hbar = 1$ is

$$H(\lambda) = \frac{p^2}{2m} + \frac{1}{2}m\omega(x - \lambda)^2 \quad (57)$$

and is parameterized by the external parameter λ , which translates the minimum of the harmonic well. This motivates introducing the translated raising and lowering operators

$$a_\lambda = \sqrt{\frac{m\omega}{2}} \left(x - \lambda + \frac{ip}{m\omega} \right), \quad (58)$$

$$a_\lambda^\dagger = \sqrt{\frac{m\omega}{2}} \left(x - \lambda - \frac{ip}{m\omega} \right), \quad (59)$$

which when substituted into the Hamiltonian (57) lead to the simplified expression

$$H(\lambda) = \omega(a_\lambda^\dagger a_\lambda + 1/2). \quad (60)$$

To do work on the oscillator, we vary λ according to a protocol $\Lambda = \{\lambda_t\}_{t=0}^T$ from $t = 0$ to T . In order to use the effective dynamics outlined in section 4, we assume that the driving is not too fast, $\dot{\lambda}_t dt \ll 1$. For notational simplicity, we will denote the translated raising and lowering operators at time t when the external parameter has value λ_t as $a_t \equiv a_{\lambda_t}$ and $a_t^\dagger \equiv a_{\lambda_t}^\dagger$.

The surroundings are composed of two distinct sequences of two-level atoms, which will mimic two thermal reservoirs at inverse temperatures β and β' . Each atom of the β (β') reservoir has ground state $|g\rangle$ ($|g'\rangle$) and excited state $|e\rangle$ ($|e'\rangle$), prepared with the Boltzmann weight $p_e/p_g = e^{-\beta\omega}$ ($p'_e/p'_g = e^{-\beta'\omega}$). The interaction is

$$V(\lambda) = h(a_\lambda \sigma^\dagger + a_\lambda^\dagger \sigma), \quad (61)$$

where $\sigma = |g\rangle\langle e|$ for the β reservoir or $\sigma = |g'\rangle\langle e'|$ for the atoms at β' .

With this setup, there are four jump operators, two for the β reservoir,

$$L_{eg}(\lambda_t) = \sqrt{gp_g}a_t, \quad L_{ge}(\lambda_t) = \sqrt{gp_e}a_t^\dagger, \quad (62)$$

and two for the β' reservoir,

$$L'_{eg}(\lambda_t) = \sqrt{gp'_g}a_t \quad L'_{ge}(\lambda_t) = \sqrt{gp'_e}a_t^\dagger. \quad (63)$$

Each pair satisfies detailed balance (29):

$$L_{eg}(\lambda) = L_{ge}^\dagger(\lambda)e^{\beta\omega/2}, \quad L'_{eg}(\lambda) = [L'_{ge}(\lambda)]^\dagger e^{\beta'\omega/2}, \quad (64)$$

where we can identify the entropy production per jump in the β reservoir $\Delta s_{eg} = \beta\omega$ and in the β' reservoir $\Delta s'_{eg} = \beta'\omega$, as the heat transferred to the reservoir divided by the temperature, as expected for a thermal reservoir.

Furthermore, these dynamics support a unique stationary state for each fixed λ ,

$$\pi_\lambda = \frac{1}{Z_\lambda} e^{-\beta_{\text{eff}} H(\lambda)}, \quad (65)$$

where $Z_\lambda = \text{Tr} \exp[-\beta_{\text{eff}} H(\lambda)]$ and

$$\beta_{\text{eff}} = -(1/\omega) \ln [(p_e + p'_e)/(p_g + p'_g)]. \quad (66)$$

Even though π_λ (65) resembles an equilibrium density matrix, the oscillator is not in equilibrium as heat flows through the system from the hotter to cooler reservoir. The associated dual jump operators, which are obtained by substituting (62), (63) and (65) into (41), are

$$L_{ge}^+(\lambda) = e^{\beta_{\text{eff}}\omega/2} L_{ge}^\dagger(\lambda), \quad L_{ge}^-(\lambda) = e^{-\beta_{\text{eff}}\omega/2} L_{ge}^\dagger(\lambda) \quad (67)$$

and

$$[L'_{ge}(\lambda)]^+ = e^{\beta_{\text{eff}}\omega/2} [L'_{ge}(\lambda)]^\dagger, \quad [L'_{ge}(\lambda)]^- = e^{-\beta_{\text{eff}}\omega/2} [L'_{ge}(\lambda)]^\dagger. \quad (68)$$

Notice that despite the harmonic oscillator being infinite dimensional, the dual operators are proportional to the original jump operators, allowing us to still consider the adiabatic and nonadiabatic entropy productions.

With this setup it is now straightforward to determine expressions for the nonadiabatic and adiabatic entropy productions. The forms are most suggestive in terms of the heat flow into the β (β') thermal reservoir along the trajectory γ , $q[\gamma]$ ($q'[\gamma]$). Combining (64), (67), (49) and (50), we have

$$\Delta s_a[\gamma] = (\beta - \beta_{\text{eff}})q[\gamma] + (\beta' - \beta_{\text{eff}})q'[\gamma], \quad (69)$$

$$\Delta s_{\text{na}}[\gamma] = \Delta s[\gamma] + \beta_{\text{eff}}(q[\gamma] + q'[\gamma]). \quad (70)$$

For a linear driving with rate ν , $\lambda_t = \nu t$, the system relaxes to a steady state in the long time limit, because in the co-moving frame the system appears at rest. In this steady state, entropy is continually being produced. It is then more informative to analyze the rate of entropy production. In this case, the system entropy change $\Delta s[\gamma]$ vanishes on average, energy conservation guarantees that the average rates of heat flow balance, $\dot{Q} = -\dot{Q}'$ and the average entropy production rates become $\dot{S}_{\text{na}} = 0$ and $\dot{S}_{\text{tot}} = \dot{S}_a = \Delta\beta \dot{Q}$, where $\Delta\beta = \beta - \beta'$.

7. Conclusion

For a wide class of open quantum systems evolving along quantum jump trajectories, we have established formulae for the trajectory-dependent total (40), adiabatic (49) and nonadiabatic (50) entropy productions by means of detailed fluctuation theorems. To arrive at these formulae, we used the continuous measurement framework in which each environment interacts with the system for a short time τ . To achieve this limit, we required that the coupling strength scale as $h \sim 1/\sqrt{\tau}$. Thus, as $\tau \rightarrow 0$ the coupling becomes infinite, yet the effect on the system remains small. A more physical limit where the coupling is finite is the weak coupling limit [21], where h is small and the interaction time is long. Unfortunately, the weak-coupling limit applies to a more restrictive class of protocols. To these authors knowledge only periodic [33], linear [14] and slow [34] driving have been successfully incorporated. Therefore, despite the unphysical nature of the continuous measurement framework, we can consider a larger variety of nonequilibrium drivings.

The key to our analysis is the local detailed balance relation (29), connecting entropy production to a symmetry of the jump operators. This relation is a natural consequence

of the time-reversal symmetry of the underlying microscopic dynamics. Often in classical statistical thermodynamics local detailed balance is considered a minimal requirement for a consistent thermodynamic description [35]. Similarly, one could take (29) as a starting point for a consistent description of the thermodynamics of jump trajectories. Beyond the classical regime, this relation holds even when the surroundings are coherent in the energy eigenbasis, leading to the appearance of a quantum thermodynamic force F (31). Unfortunately, there is no clear connection between this force and the change in Shannon entropy of the surroundings as one would hope. In general, it remains an open problem to interpret the environment entropy production (30) for any nonthermal environment. We suspect that if we embed such a nonthermal environment in a larger thermal super-reservoir, then (30) may bound the physical entropy production in the super-reservoir. This intuition is supported by the analysis of Scully [30] and Zubairy [36] showing that the work necessary to create the coherent reservoir exploited by the photo-Carnot engine always exceeds the useful work extracted from the engine. Despite this shortcoming, the introduction of F still allows for a consistent description of irreversibility—the distinguishability of the forward and reverse processes—through the total entropy production.

Our analysis has focused on entropy production and its fluctuations. However, the setup we have presented here can be extended to incorporate a variety fluctuation relations. The key observation is that instead of initializing the reverse process with the final distribution of the forward process, P_b , we can use any other probability distribution \tilde{P}_b . Then the trajectory functional $\mathcal{R}[\gamma] = \ln(\mathcal{P}[\gamma|a]/\tilde{\mathcal{P}}[\tilde{\gamma}|\tilde{b}]) + \ln P_a/\tilde{P}_b$ will satisfy an integral and detailed fluctuation theorem. By making various choices for the operator B and \tilde{P}_b , we can arrive at any of a collection of fluctuation relations as in the classical case [37, 38], see for example the discussion in [14] on work fluctuation relations.

In contrast to the trajectory analysis we have performed, Chetrite and Mallick [28] have recently predicted an integral fluctuation theorem for the nonadiabatic entropy production for driven quantum Markov semigroups. Their result is based on quantum multi-time correlation functions and makes no explicit mention of trajectories. While we expect that their results and ours are closely related, the precise relationship is still an open question that deserves further analysis.

To conclude, we must comment on the classical nature of the quantum jump trajectories we have discussed. As merely a collection of classical measurement outcomes, they are classical trajectories. However, each trajectory can be mapped to a stochastic path through Hilbert space traced out by the conditioned wave vector of the system [14]. Such an identification is possible, since the interaction in (4) has only one term that mediates each transition between environment energy eigenspaces. As a result, the jump operations in (18) map pure states to pure states, allowing an evolution described completely in terms of vectors. For a more general interaction, such an identification would not be possible. Instead, one may consider the evolution of the conditioned density matrix as a quantum trajectory.

Despite the classical nature of the measurement trajectories, quantum effects still manifest themselves in their statistics. In particular, such quantum influence is observed when there is coherence in the surroundings, or when the driving is rapid enough to cause nonadiabatic transitions between energy eigenstates of the system. Even more opportunities exist to use the framework outlined here to study the thermodynamics of a variety of purely quantum phenomena such as decoherence, entanglement or measurement.

Acknowledgments

JMH is supported financially by the National Science Foundation (USA) International Research Fellowship under grant no. OISE-1059438 and by ARO MURI grant W911NF-11-1-0268. JMRP is supported by the Spanish Government under grant no. FIS2011-22644.

Appendix A. Effective dynamics for short interactions

In this appendix, we demonstrate how to arrive at the effective dynamics outlined in section 4.1 when the interaction time is short $h\tau \ll 1$ and the coupling strength scales as $h = \sqrt{g/\tau}$. The technique we apply here is adapted from [9, 20].

To begin, we solve the Schrödinger equation for the time-evolution operator $U(t, t_0)$ during one τ -interval starting at $t = t_0$ for small times $h\tau \ll 1$:

$$\frac{\partial U}{\partial t} = -i(H(\lambda_t) + H_E + V(\lambda_t))U, \quad (\text{A.1})$$

with initial condition $U(t_0, t_0) = I$. This is facilitated by entering the interaction picture by multiplying U by the operator

$$K(t, t_0) = K_S(t, t_0)K_E(t, t_0) \equiv \mathcal{T} \exp \left[-i \int_{t_0}^t ds H(\lambda_s) \right] \exp[-i(t - t_0)H_E] \quad (\text{A.2})$$

to get $U_I(t, t_0) = K^\dagger(t, t_0)U(t, t_0)$, which evolves according to

$$\frac{\partial U_I}{\partial t} = -iV_I(t)U_I, \quad (\text{A.3})$$

where $V_I(t) = K^\dagger(t, t_0)V(\lambda_t)K(t, t_0)$. A formal solution to (A.3) is given by the series

$$U_I(t_0 + \tau, t_0) = I + \sum_{n=1}^{\infty} (-i)^n \int_{t_0}^{\tau} ds_n \cdots \int_{t_0}^{s_2} ds_1 V_I(s_n) \cdots V_I(s_1), \quad (\text{A.4})$$

whose approximate solution for small times τ is

$$U_I(t_0 + \tau, t_0) \approx I - i\tau V_I(t_0) - \frac{\tau^2}{2}(V_I^2(t_0) + i\partial_t V_I(t_0)). \quad (\text{A.5})$$

Equation (A.5) now allows us to deduce the short time behavior for the quantum operation \mathcal{E}_{ji} when the environment transitions from \mathcal{H}_i to a *different* eigenspace \mathcal{H}_j . Exploiting the property that each R only connects one pair of energy eigenspaces of the environment, and $[K_E, H_E] = 0$, gives

$$\mathcal{E}_{ji}(\rho) \approx \tau^2 K_S(t_0 + \tau, t_0) \text{Tr}_E[\Pi_j V_I(t_0)\rho \otimes p_i r_i V_I^\dagger(t_0)] K_S^\dagger(t_0 + \tau, t_0). \quad (\text{A.6})$$

Substituting in the definitions of V in (4) and L_{ji} in (19), and $h = \sqrt{g/\tau}$ leads to

$$\mathcal{E}_{ji}(\rho) \approx \tau K_S(t_0 + \tau, t_0) L_{ji}(\lambda_{t_0}) \rho L_{ji}^\dagger(\lambda_{t_0}) K_S^\dagger(t_0 + \tau, t_0). \quad (\text{A.7})$$

Similarly, when the environment does not transition

$$\mathcal{E}_{ii}(\rho) \approx K_S(t_0 + \tau, t_0) p_i \rho K_S^\dagger(t_0 + \tau, t_0) \quad (\text{A.8})$$

$$- \frac{\tau^2}{2} K_S(t_0 + \tau, t_0) \text{Tr}_E \left[\Pi_i \left(V_I^2(t_0) \rho \otimes p_i r_i + \rho \otimes p_i r_i (V_I^\dagger(t_0))^2 \right) \right] K_S^\dagger(t_0 + \tau, t_0) \quad (\text{A.9})$$

$$\approx K_S(t_0 + \tau, t_0) \left[p_i \rho - \frac{\tau}{2} \left\{ \sum_l L_{li}^\dagger(\lambda_{t_0}) L_{li}(\lambda_{t_0}), \rho \right\} \right] K_S^\dagger(t_0 + \tau, t_0), \quad (\text{A.10})$$

where for two operators O and O' , $\{O, O'\} = OO' + O'O$ is the anticommutator.

We now investigate the evolution during a small time interval $dt = M\tau$ with $M \gg 1$, during which many environments interact with the system, but the probability to observe a jump remains small. This coarse-graining allows us to describe the dynamics as a Poisson process, where the jumps are rare and occur instantaneously on the time scale $\tau \ll dt$. Furthermore, we assume that during dt the system dynamics are negligible, and we can approximate $K_S(t_0 + dt, t_0) \approx I - iH(\lambda_{t_0}) dt$.

Consider a $dt = M\tau$ window from $t = t_0$ to $t_0 + dt$ when a jump is observed, say $i \rightarrow j$. We cannot know precisely which of the M environments jumped. Therefore, to correctly predict the change in the system, we must sum over all possibilities

$$\mathcal{J}_{ji}(\rho) = \sum_{k=1}^M \sum_{i_M} \mathcal{E}_{i_M i_M} \cdots \mathcal{E}_{j k i_k} \cdots \sum_{i_1} \mathcal{E}_{i_1 i_1}(\rho) \quad (\text{A.11})$$

$$\approx L_{ji}(\lambda_{t_0}) \rho L_{ji}^\dagger(\lambda_{t_0}) dt, \quad (\text{A.12})$$

keeping only terms lowest order in dt , and remembering that the external parameters λ do not change significantly during dt . The probability for this event is

$$P_{ji} = \text{Tr}_S[\mathcal{J}_{ji}(\rho)] = \langle L_{ji}^\dagger(\lambda_{t_0}) L_{ji}(\lambda_{t_0}) \rangle dt, \quad (\text{A.13})$$

where $\langle \cdot \rangle = \text{Tr}_S[\cdot \rho]$. Equation (A.13) is of order dt signaling that the jump statistics are described by a Poisson process. Similarly, during an interval when no jumps are detected in any of the M environments the effect on the system is given by

$$\mathcal{U}_{t_0+dt, t_0}(\rho) = \sum_{i_M} \mathcal{E}_{i_M i_M} \cdots \sum_{i_1} \mathcal{E}_{i_1 i_1}(\rho) \quad (\text{A.14})$$

$$\approx \left[K_S(t_0 + dt, t_0) - \frac{dt}{2} \sum_{ji} L_{ji}^\dagger(\lambda_{t_0}) L_{ji}(\lambda_{t_0}) \right] \rho \left[K_S^\dagger(t_0 + dt, t_0) - \frac{dt}{2} \sum_{ji} L_{ji}^\dagger(\lambda_{t_0}) L_{ji}(\lambda_{t_0}) \right] \quad (\text{A.15})$$

$$\approx [I - i dt H_{\text{eff}}(\lambda_{t_0})] \rho [I + i dt H_{\text{eff}}^\dagger(\lambda_{t_0})] \quad (\text{A.16})$$

$$\approx U_{\text{eff}}(t_0 + dt, t_0) \rho U_{\text{eff}}^\dagger(t_0 + dt, t_0), \quad (\text{A.17})$$

where we have expanded $K_S(t_0 + dt, t_0) \approx I - iH(\lambda_{t_0}) dt$ and substituted in the definitions of H_{eff} (22) and U_{eff} (21). The probability of not observing any jumps is

$$P_{\text{no-jump}} = \text{Tr}_S[\mathcal{U}_{t_0+dt, t_0}(\rho)] \approx 1 - \sum_{ji} \langle L_{ji}^\dagger(\lambda_{t_0}) L_{ji}(\lambda_{t_0}) \rangle dt, \quad (\text{A.18})$$

which confirms that the dynamics are governed by a compound Poisson process for the different possible transitions between energy eigenspaces. Equations (A.12) and (A.17) demonstrate that the effective equations of motion are governed by U_{eff} between jumps and the operators L_{ji} at jumps.

In the reverse process, the same arguments lead to a jump quantum operation at time t :

$$\tilde{\mathcal{J}}_{ji}(\rho) = gp_i \text{Tr}_E[R_{ji}^\dagger R_{ji} \tilde{r}_i] S_{ji}(\tilde{\lambda}_t) \rho S_{ji}^\dagger(\tilde{\lambda}_t) dt \equiv \tilde{L}_{ji}(\tilde{\lambda}_t) \rho \tilde{L}_{ji}^\dagger(\tilde{\lambda}_t) dt. \quad (\text{A.19})$$

To arrive at (27) for \tilde{L}_{kl} , we first separate the time-reversal operator $\Theta = \theta_S \otimes \theta_E$ into the time-reversal operator on the system θ_S and environment θ_E . Then,

$$\tilde{\mathcal{J}}_{ji}(\rho) = gp_i \text{Tr}_E[R_{ji} S_{ji}(\tilde{\lambda}_t) \rho \otimes \theta_E r_i \theta_E^{-1} S_{ji}^\dagger(\tilde{\lambda}_t) R_{ji}^\dagger] dt. \quad (\text{A.20})$$

and its time-reversal is

$$\theta_S \tilde{\mathcal{J}}_{ji}(\theta_S \rho \theta_S^{-1}) \theta_S^{-1} = gp_i \text{Tr}_E[\Theta R_{ji} S_{ji}(\tilde{\lambda}_t) \Theta \rho \otimes r_i \Theta^{-1} S_{ji}^\dagger(\tilde{\lambda}_t) R_{ji}^\dagger \Theta^{-1}], \quad (\text{A.21})$$

after inserting a $\theta_E \theta_E^{-1} = I$ outside the the time-reversal invariant environment operators R_{ji} . Noting the time-reversal invariance of the interaction $\Theta V \Theta = V$, we arrive at

$$\theta_S \tilde{\mathcal{J}}_{ji}(\theta_S \rho \theta_S^{-1}) \theta_S^{-1} = gp_i \text{Tr}_E[R_{ji}^\dagger R_{ji} r_i] S_{ji}(\tilde{\lambda}_t) \rho S_{ji}^\dagger(\tilde{\lambda}_t), \quad (\text{A.22})$$

from which it is straightforward to arrive at (27) by comparing with (A.19).

Appendix B. Operators for dual quantum Markov processes

The dual process is defined such that $\mathcal{P}_{\text{st}}^+[\tilde{\gamma}] = \mathcal{P}_{\text{st}}[\gamma]$. To identify the jump operators L_{kl}^+ and effective time-evolution operator U_{eff}^+ of the dual process, we begin by analyzing $\mathcal{P}_{\text{st}}[\gamma]$. Since λ is fixed throughout the calculation we will suppress it in the notation. For our purposes here it is sufficient to consider a trajectory with only one jump $\gamma = \{e_k; t_1, i \rightarrow j; e_l\}$ between two eigenstates $|e_k\rangle$ and $|e_l\rangle$ of the stationary density $\pi = \sum_n p_n^{\text{st}} |e_n\rangle \langle e_n|$:

$$\mathcal{P}_{\text{st}}[\gamma] = |\langle e_l | U_{\text{eff}}(T, t_1) L_{ji} U_{\text{eff}}(t_1, 0) | e_k \rangle|^2 p_k^{\text{st}}. \quad (\text{B.1})$$

First, we note that since π is positive-definite it has an inverse π^{-1} and square root $\pi^{1/2}$. Therefore, we can rewrite (B.1) as

$$\mathcal{P}_{\text{st}}^+[\gamma] = |\langle e_l | \pi^{-1/2} U_{\text{eff}}(T, t_1) L_{ji} U_{\text{eff}}(t_1, 0) \pi^{1/2} | e_k \rangle|^2 p_l^{\text{st}}. \quad (\text{B.2})$$

Next, following Crooks [17], we insert between each pair of operators the identity operator $I = \pi^{1/2} \pi^{-1/2}$,

$$\mathcal{P}_{\text{st}}[\gamma] = |\langle e_l | \pi^{-1/2} U_{\text{eff}}(T, t_1) \pi^{1/2} \pi^{-1/2} L_{ji} \pi^{1/2} \pi^{-1/2} U_{\text{eff}}(t_1, 0) \pi^{1/2} | e_k \rangle|^2 p_l^{\text{st}}, \quad (\text{B.3})$$

followed by $I = \Theta \Theta^{-1}$,

$$\begin{aligned} \mathcal{P}_{\text{st}}[\gamma] &= |\langle e_l | \Theta (\Theta^{-1} \pi^{-1/2} U_{\text{eff}}(T, t_1) \pi^{1/2} \Theta) (\Theta^{-1} \pi^{-1/2} L_{ji} \pi^{1/2} \Theta) \\ &\quad \times (\Theta^{-1} \pi^{-1/2} U_{\text{eff}}(t_1, 0) \pi^{1/2} \Theta) \Theta^{-1} | e_k \rangle|^2 p_l^{\text{st}}. \end{aligned} \quad (\text{B.4})$$

Finally, we use the anti-unitarity of Θ to flip the order of the operators

$$\begin{aligned} \mathcal{P}_{\text{st}}[\gamma] &= |\langle \tilde{e}_k | (\Theta \pi^{1/2} U_{\text{eff}}^\dagger(t_1, 0) \pi^{-1/2} \Theta^{-1}) (\Theta \pi^{1/2} L_{ji}^\dagger \pi^{-1/2} \Theta^{-1}) \\ &\quad \times (\Theta \pi^{1/2} U_{\text{eff}}^\dagger(T, t_1) \pi^{-1/2} \Theta^{-1}) | \tilde{e}_l \rangle|^2 p_l^{\text{st}}, \end{aligned} \quad (\text{B.5})$$

recalling that $|\tilde{e}_n\rangle = |\Theta e_n\rangle$. Comparing with the dual process

$$\mathcal{P}_{\text{st}}^+[\tilde{\gamma}] = |\langle \tilde{e}_k | U_{\text{eff}}^+(T, T - t_1) L_{ij}^+ U_{\text{eff}}^+(T - t_1, 0) | \tilde{e}_l \rangle|^2 p_l^{\text{st}}, \quad (\text{B.6})$$

we arrive at (41) and (42), reprinted here for convince

$$L_{ij}^+ = \Theta \pi^{1/2} L_{ji}^\dagger \pi^{-1/2} \Theta^{-1} \quad (\text{B.7})$$

and

$$U_{\text{eff}}^+(t, s) = \Theta \pi^{1/2} U_{\text{eff}}^\dagger(T - s, T - t) \pi^{-1/2} \Theta^{-1}. \quad (\text{B.8})$$

Equation (46) for U_{eff}^+ can be derived by first differentiating with time (B.8)

$$\frac{\partial}{\partial t} U_{\text{eff}}^+(t, s) = \Theta \pi^{1/2} \frac{\partial}{\partial t} [U_{\text{eff}}^\dagger(T - t, t - s)]^{-1} \pi^{-1/2} \Theta^{-1}, \quad (\text{B.9})$$

$$= \Theta \pi^{1/2} (iH_{\text{eff}}^\dagger) [U_{\text{eff}}^\dagger(T - t, t - s)]^{-1} \pi^{-1/2} \Theta^{-1}, \quad (\text{B.10})$$

$$= -iH_{\text{eff}}^+ U_{\text{eff}}^+(t, s), \quad (\text{B.11})$$

where

$$H_{\text{eff}}^+ = \Theta \pi^{1/2} H_{\text{eff}}^\dagger \pi^{-1/2} \Theta^{-1} = \Theta \pi^{1/2} \left[H + \frac{i}{2} \sum_{kl} L_{kl}^\dagger L_{kl} \right] \pi^{-1/2} \Theta^{-1}. \quad (\text{B.12})$$

Finally, in the privileged representation $[H, \pi] = [\sum_{kl} L_{kl}^\dagger L_{kl}, \pi] = 0$ (44), H and L_{kl} are assumed time-reversal invariant and $\Theta i = -i\Theta$ implying that $H_{\text{eff}}^+ = H_{\text{eff}}$. Consequently, U_{eff}^+ and U_{eff} satisfy the same differential equation (21) with the same initial conditions and therefore must be equal.

References

- [1] de Groot S R and Mazur P 1984 *Non-Equilibrium Thermodynamics* (New York: Dover)
- [2] Esposito M and Van den Broeck C 2010 *Phys. Rev. Lett.* **104** 090601
- [3] Hatano T 1999 *Phys. Rev. E* **60** R5017–20
- [4] Hatano T and Sasa S I 2001 *Phys. Rev. Lett.* **86** 3463–6
- [5] Speck T and Seifert U 2005 *J. Phys. A: Math. Gen.* **38** L581–8
- [6] Seifert U 2008 *Eur. Phys. J. B* **64** 423–31
- [7] Esposito M, Harbola U and Mukamel S 2009 *Rev. Mod. Phys.* **81** 1665–702
- [8] Campisi M, Hänggi P and Talkner P 2011 *Rev. Mod. Phys.* **83** 771–91
- [9] Kist T, Orszag M, Brun T A and Davidovich L 1999 *J. Opt. B: Quantum Semiclass. Opt.* **1** 251–63
- [10] Spehner D and Orszag M 2002 *J. Math. Phys.* **43** 3511–37
- [11] Attal S and Pautrat Y 2006 *Ann. Inst. Henri Poincaré A* **7** 59–104
- [12] Attal S and Joye A 2007 *J. Stat. Phys.* **127** 1241–83
- [13] Santos M and Carvalho A 2011 *Europhys. Lett.* **94** 64003
- [14] Horowitz J M 2012 *Phys. Rev. E* **85** 031110
- [15] De Roeck W and Maes C 2006 *Rep. Math. Phys.* **18** 619–53
- [16] Dereziński J, De Roeck W and Maes C 2008 *J. Stat. Phys.* **131** 341–56
- [17] Crooks G E 2008 *Phys. Rev. A* **77** 034101
- [18] Hekking F W J and Pekola J P 2013 Quantum jump approach for work and dissipation in a two-level system arXiv:1305.5207v1
- [19] Scully M O, Zubairy M S, Agarwal G S and Walther H 2003 *Science* **299** 862–4

- [20] Ueda M, Imoto N, Nagaoka H and Ogawa T 1992 *Phys. Rev. A* **46** 2859–69
- [21] Breuer H P and Petruccione F 2009 *The Theory of Open Quantum Systems* (Oxford: Clarendon)
- [22] Andrieux D, Gaspard P, Monnai T and Tasaki S 2009 *New J. Phys.* **11** 043014
- [23] Jacobs K and Steck D 2006 *Contemp. Phys.* **47** 279
- [24] Nechita I and Pellegrini C 2009 *Confluentes Math.* **1** 249–89
- [25] Wiseman H M 1996 *Quantum Semiclass. Opt.* **8** 205–22
- [26] Fagnola F and Umanità V 2007 *Infinite Dimens. Anal. Quantum Probab. Relat. Top.* **10** 335–63
- [27] Fagnola F and Umanità V 2008 *Math. Notes* **84** 108–15
- [28] Chetritie R and Mallick K 2012 *J. Stat. Phys.* **148** 480–501
- [29] Esposito M and Van den Broeck C 2010 *Phys. Rev. E* **82** 011143
- [30] Scully M O 2002 Extracting work from a single heat bath via vanishing quantum coherence: II. Microscopic model *First Int. Conf. on Quantum Limits to the Second Law* ed D P Sheehan (New York: AIP) pp 83–91
- [31] Rostovtsev Y V, Saryianni Z E and Scully M O 2003 *Laser Phys.* **13** 375–85
- [32] Lutz E and Dillenschneider R 2009 *Europhys. Lett.* **88** 50003
- [33] Breuer H P and Petruccione F 1997 *Phys. Rev. A* **55** 3101–16
- [34] Alicki R 1979 *J. Phys. A: Math. Gen.* **12** L103
- [35] Seifert U 2012 *Rep. Prog. Phys.* **75** 126001
- [36] Zubairy M S 2002 The photo-carno cycle: The preparation energy for atomic coherence *First Int. Conf. on Quantum Limits to the Second Law* ed D P Sheehan (New York: AIP) pp 92–7
- [37] Harris R J and Schütz G M 2007 *J. Stat. Mech.: Theor. Exp.* P07020
- [38] Seifert U 2005 *Phys. Rev. Lett.* **95** 040602